stationary solution corresponds to asymmetrical traffic with $C_{ij} = \frac{q\phi}{\nu} \pm \sqrt{D^2}$ and $C_{i'j} = \frac{q\phi}{\nu} \mp \sqrt{D^2}$. If $\gamma = 0$, this situation is given for $q\phi/\nu > k$. If $q\phi/\nu \leq k$, that is, if the pheromone concentration is too low, the ants choose both branches at random, corresponding to a symmetrical distribution (Fig. 4a). Case (2): when pushing is taken into account with $\gamma > 0$, the organization of traffic changes considerably: the asymmetrical solution can no longer be established as soon as $D^2 < 0$ for large traffic volumes $\phi$ (Fig. 4b). In this case, symmetrical traffic is expected with $C_{ij} = q\phi/\nu$ and $\Phi_{ij} = \phi/2$ for both branches $i$ and choice points $j$. Therefore, high traffic volumes can be maintained and none of the branches is preferred in spite of the competitive effect due to the accumulation of pheromone on both branches. Moreover, the model implies that the outbound flow $\Phi_{i1}$ and the nestbound flow $\Phi_{i2}$ are equal, indicating that one-way flows are not required to maintain a high traffic volume[23]. These analytical results have been confirmed by Monte Carlo simulations (see Fig. 4c, d). Our simulations have also demonstrated that if pushed ants, instead of moving to the other branch, made a U-turn and returned in the direction they had been coming from, the overall flow of ants crossing the bridge was affected by the branch width and no shift to symmetrical traffic was observed.

The traffic organization in ants can be called optimal. The overall flow on branch $i$ behind choice point $j$ is given by $\Phi_{ij} = w\rho_{ij}V_{ij} \leq \phi$, where $\rho_{ij}$ denotes the density of ants. Their average speed is theoretically estimated by $V_{ij} \approx V_m(1 - a\Phi_{ij'}/w)$, where $V_m$ denotes the average maximum speed and $a\Phi_{ij'}/w$ is again the proportion of decelerated ants. For the symmetry-restoring transition with $D^2 = 0$, equation (7) requires $a\gamma\phi/w < 1/3$, which implies $V_{ij} > V_m[1 - 1/(3\gamma)] \approx 0.42V_m$. However, according to the empirical speed–density relation by Burd *et al.*[23], the maximum flow (the capacity) is only reached at the smaller speed $V_{ij} = V_m[1 - 1/(n+1)] \approx 0.39V_m$. Although the empirical value $n \approx 0.64$ was determined for another ant species, the values for *L. niger* should be comparable. This shows that the symmetry-restoring transition occurs before the maximum flow is reached. The strict inequality also implies capacity reserves and a limitation of the density-related speed reduction. A marginal reduction in speed, however, would not favour symmetrical traffic because of the benefits of using a single trail. First, a more concentrated trail provides a better orientation guidance and a stronger arousal stimulus[24]. Second, a higher density of ants enhances information exchange and supports a better group defence[25].

We have demonstrated the surprising functionality of collisions among ants to keep up the desired flow level by generation of symmetrical traffic. Pushing behaviour may be considered an optimal behaviour to maintain a high rate of food return to the nest. It would not be required in most models of ideal free distribution (IDF)[26], as they neglect effects of inter-attraction. The balancing between cohesive and dispersive forces avoids a dysfunctional degree of aggregation and supports an optimal accessibility of space at minimal costs allowing an efficient construction, maintenance and use of infrastructures. This mechanism appears to be generic in nature, in particular in group-living organisms. For example, inhibitory interactions at overcrowded building sites in termites allow a smooth growth of the nest structure[27]. In the development of urban agglomerations such interactions help to maintain the coexistence of distinct cities[28], and in vehicle traffic they determine the choice of longer, less congested routes. The mechanism also suggests algorithms for the routeing of data traffic in networks. □

Received 11 December 2003; accepted 13 January 2004; doi:10.1038/nature02345.

1. Helbing, D. Traffic and related self-driven many-particle systems. *Rev. Mod. Phys.* **73,** 1067–1141 (2001).
2. Camazine, S., *et al. Self-organized Biological Systems* (Princeton Univ. Press, Princeton, 2001).
3. Bonabeau, E., Dorigo, M. & Theraulaz, G. Inspiration for optimization from social insect behaviour. *Nature* **406,** 39–42 (2000).
4. Bonabeau, E., Dorigo, M. & Theraulaz, G. *Swarm Intelligence: From Natural to Artificial Systems* (Oxford Univ. Press, New York, 1999).
5. Burd, M. & Aranwela, N. Head-on encounter rates and walking speed of foragers in leaf-cutting ant traffic. *Insectes Soc.* **50,** 3–8 (2003).
6. Couzin, I. D. & Franks, N. R. Self-organized lane formation and optimized traffic flow in army ants. *Proc. R. Soc. Lond. B* **270,** 139–146 (2003).
7. Parrish, J. K. & Hamner, W. K. *Animal Groups in Three Dimensions* (Cambridge Univ. Press, Cambridge, UK, 1997).
8. Krause, J. & Ruxton, D. *Living in Groups* (Oxford Univ. Press, Oxford, UK, 2002).
9. Galef, B. G. Jr & Buckley, L. L. Using foraging trails by Norway rats. *Anim. Behav.* **51,** 765–771 (1996).
10. Fitzgerald, T. D. *The Tent Caterpillars* (Cornell Univ. Press, Ithaca, NY, 1995).
11. Erlandson, J. & Kostylev, V. Trail following, speed and fractal dimension of movement in a marine prosobranch, *Littorina littorea*, during a mating and a non-mating season. *Mar. Biol.* **122,** 87–94 (1995).
12. Traniello, J. F. A. & Robson, S. K. in *Chemical Ecology of Insects* (eds Cardé, R. T. & Bell, W.) 241–286 (Chapman & Hall, New York, 1995).
13. Miura, T. & Matusmoto, T. Open-air litter foraging in the nasute termite *Longipeditermes longipes* (Isoptera: Termitidae). *J. Insect Behav.* **11,** 179–189 (1998).
14. Helbing, D., Keltsch, J. & Molnár, P. Modelling the evolution of human trail systems. *Nature* **388,** 47–50 (1997).
15. Edelstein-Keshet, L. W., Ermentrout, J. & Bard, G. Trail following in ants: individual properties determine population behaviour. *Behav. Ecol. Sociobiol.* **36,** 119–133 (1995).
16. Schweitzer, F. *Brownian Agents and Active Particles. Collective Dynamics in the Natural and Social Sciences* (Springer, Berlin, 2003).
17. Wilson, E. O. Chemical communication among workers of the fire ant *Solenopsis saevissima* (Fr. Smith). 1. The organization of mass-foraging. *Anim. Behav.* **10,** 134–147 (1962).
18. Hölldobler, B. & Wilson, E. O. *The Ants* 265–279 (The Belknap Press of Harvard Univ. Press, Cambridge, MA, 1990).
19. Beckers, R., Deneubourg, J. L. & Goss, S. Trails and U-turns in the selection of a path by the ant *Lasius niger. J. Theor. Biol.* **159,** 397–415 (1992).
20. Goss, S., Aron, S., Deneubourg, J. L. & Pasteels, J. M. Self-organized shortcuts in the Argentine ant. *Naturwissenschaften* **76,** 579–581 (1989).
21. Pasteels, J. M., Deneubourg, J. L. & Goss, S. in *From Individual to Collective Behaviour in Social Insects* (eds Pasteels, J. M. & Deneubourg, J. L.) Experientia suppl. Vol. 54, 155–175 (Birkhäuser, Basel, 1987).
22. Helbing, D. & Platkowski, T. Drift- or fluctuation-induced ordering and self-organization in driven many-particle systems. *Europhys. Lett.* **60,** 227–233 (2002).
23. Burd, M. *et al.* Traffic dynamics of the leaf-cutting ant *Atta cephalotes*. *Am. Nat.* **159,** 283–293 (2002).
24. Calenbuhr, V. *et al.* A model for osmotropotactic orientation. II. *J. Theor. Biol.* **158,** 395–407 (1992).
25. Feener, D. H. & Moss, K. A. G. Defense against parasites by hitchhikers in leaf-cutting ants: a quantitative assessment. *Behav. Ecol. Sociobiol.* **49,** 348–356 (1990).
26. Fretwell, S. D. & Lucas, H. L. On territorial behavior and other factors influencing habitat distribution in birds. I. Theoretical development. *Acta Biotheor.* **19,** 16–36 (1970).
27. O'Toole, D. V., Robinson, P. A. & Myerscough, M. R. Self-organized criticality in termite architecture: a role for crowding in ensuring ordered nest expansion. *J. Theor. Biol.* **198,** 305–327 (1999).
28. Fujita, M., Krugman, P. & Venables, A. *The Spatial Economy–Cities, Regions, and International Trade* (MIT Press, Cambridge, MA, 1999).

**Acknowledgements** We thank G. Theraulaz and all the members of his team 'Ethology and modelization of collective behaviours' for discussions and comments on the manuscript. We also thank A. Schadschneider for discussions.

**Competing interests statement** The authors declare that they have no competing financial interests.

**Correspondence** and requests for materials should be addressed to A.D. (dussutou@cict.fr).

# Perceiving distance accurately by a directional process of integrating ground information

**Bing Wu[1], Teng Leng Ooi[2] & Zijiang J. He[1]**

[1]*Department of Psychological and Brain Sciences, University of Louisville, Louisville, Kentucky 40292, USA*
[2]*Department of Basic Sciences, Pennsylvania College of Optometry, 8360 Old York Road, Elkins Park, Pennsylvania 19027, USA*

**By itself, the absolute distance of an object cannot be accurately judged beyond 2–3 m (refs 1–3). Yet, when it is viewed with reference to a flat terrain, humans accurately judge the absolute distance of the object up to 20 m, an ability that is important for various actions[4–8]. Here we provide evidence that this is accomplished by integrating local patches of ground information into a global surface reference frame. We first show that restricting an**

**observer's visual field of view to the local ground area around the target leads to distance underestimation, indicating that a relatively wide expanse of the ground surface is required for accurate distance judgement. Second, as proof of surface integration, we show that even with the restricted view, the observer can accurately judge absolute distance by scanning local patches of the ground surface, bit by bit, from near to far, but not in the reverse direction. This finding also reveals that the surface integration process uses the near-ground-surface information as a foundation for surface representation, and extrapolation to the far ground surface around the target for accurate absolute distance computation.**

Experiment 1 examined how the visual field of view affects judged absolute distance, to show that extended ground surface is required for accurate space vision. The observer wore a pair of opaque goggles with a monocular rectangular aperture that limited the field of view to the flat grass field surrounding the target. During the trial, the observer kept his head still, judged the target distance, then closed his eyes and walked blindly to traverse the remembered target distance. Figure 1a plots the averaged distances walked, reflecting the judged absolute distances in three aperture-size conditions. When the field of view was $38.6^\circ \times 39.5^\circ$, the walked distances were accurate and similar to the full-view condition[9] (control) ($F(1,7) = 0.012$, $P = 0.916$; $F(3,21) = 0.370$, $P = 0.775$). Significantly, distance was underestimated when the field of view was reduced to $21.2^\circ \times 21.2^\circ$ ($F(1,7) = 18.267$, $P < 0.005$; $F(3,21) = 1.651$, $P = 0.208$) and $13.9^\circ \times 13.5^\circ$ ($F(1,7) = 60.857$, $P < 0.001$; $F(3,21) = 9.702$, $P < 0.001$). These findings reveal that the size of the visible field is significant in absolute distance judgement[10,11]; that is, large-scale ground-surface information (more than 21°) is essential.

To underscore the effect of field size, we next tested the prediction that a small visual field also exaggerates the error in relative length-in-depth judgement. Thus, in Experiment 2 the observers viewed an L-shaped target on the flat grass field in three aperture-size conditions (Fig. 2b). The adjustable length ($Z$) of the L-shaped target was positioned in depth, whereas its width was fixed ($W = 40.5$ cm) in the frontoparallel plane. The observer perceptually matched the $Z$ and $W$, which allowed us to compute the perceptual aspect ratio, $R$, defined as $W/Z$ (ref. 12). In this way, $R < 1$ indicates that the observer required a longer $Z$ to match $W$; that is, the relative length-in-depth of the L-shaped target is underestimated. The averaged results (Fig. 1b) show relative length-in-depth underestimation ($R < 1$) in all three aperture-size conditions. When the field size was $38.6^\circ \times 39.5^\circ$, the perceptual aspect ratios were similar to that in the full view (control) condition ($F(1,7) = 0.013$, $P = 0.914$; $F(2,14) = 0.077$, $P = 0.926$). Although such findings of depth compression are expected[6,12,13], depth compression becomes significantly larger than the full-view condition with the $21.2^\circ \times 21.2^\circ$ aperture ($F(1,7) = 17.001$, $P < 0.005$; $F(2,14) = 5.578$, $P < 0.025$), and larger still with the $13.9^\circ \times 13.5^\circ$ aperture ($F(1,7) = 60.017$, $P < 0.001$; $F(2,14) = 6.860$, $P < 0.01$). Clearly, decreasing the ground-surface view also adversely affects relative length-in-depth judgement (Fig. 1b), as it does absolute distance judgement (Fig. 1a).

Figure 2 points to a likely common basis for the findings of Experiments 1 and 2. When a patch of far ground surface (more than 2–3 m) is seen in isolation, the depth information consists mainly of texture gradient cues, which are insufficient for the visual system to code absolute distance accurately[14]. Moreover, the patch of far ground surface is perceived as slanted towards the vertical (the frontal tendency)[15–17]. Consequently, when constrained to sampling only this far surface patch, the global visual representation of the ground (grey line in Fig. 2a) is based on this far patch with a perceived slant error of $\eta$ degrees. This then compels the visual system to determine the target position on the ground on the basis of the slant surface representation.

Now that the target is represented as located on a surface with a slant error ($\eta$), whereas its angular declination ($\alpha$) is correctly perceived[3], its absolute distance, $d$, on the ground surface is obtained according to the trigonometric relationship (Fig. 2a)

$$d = DH/(H\cos\eta + D\sin\eta)$$

where $D$ and $H$ are the physical distance of the object on the ground and the observer's eye height, respectively. Thus, on the basis of this relationship, when the ground-surface representation is slanted upward (that is, $\eta > 0$), $d$ becomes smaller than $D$, leading to absolute distance underestimation. Similarly, the perceptual aspect ratio ($R$) is described by

$$R = H/[H\cos\eta + (D + Z)\sin\eta]$$

where $Z$ is the matched depth of the L-shaped target (Fig. 2b).

We applied the averaged absolute distance ($d$) and perceptual aspect ratios ($R$) data from Fig. 1a, b, respectively, into each equation above to derive the slant errors ($\eta$). As plotted in Fig. 2c, the slant errors in both absolute distance and relative length-in-depth judgements increase with decreasing field of view, even as the two sets of data differ[7] because of the compression of depth in relative length-in-depth judgement ($\eta > 0$), whereas absolute distance judgement remains accurate ($\eta = 0$) in the full-view condition[4–8,12,13]. Then, for a given test distance and visual field size, we related the derived slant errors ($\eta$) from relative length-in-depth to absolute distance judgements in a scatter plot (Fig. 2d). Clearly, a

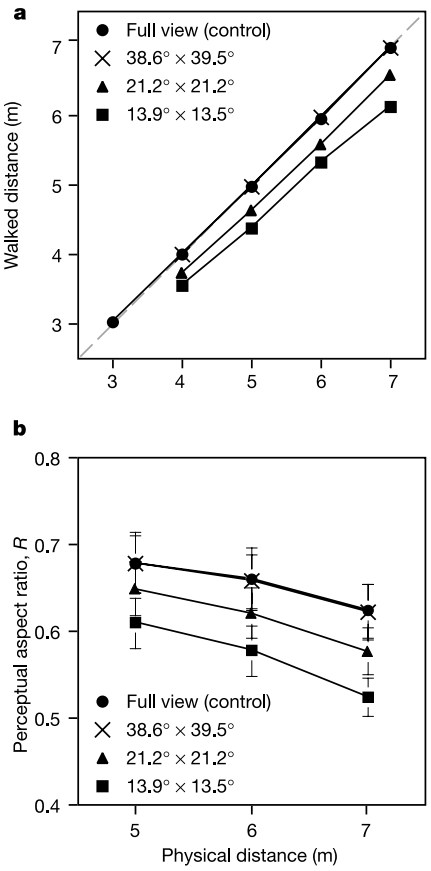


**Figure 1** The effect of visual field size on judged distance. **a**, Absolute walked distance from the blind-walking task is plotted as a function of the physical distance. **b**, Judged relative length-in-depth from the perceptual matching task, defined as the perceptual aspect ratio ($R$) of the L-shaped target, is plotted as a function of the physical distance. Each symbol represents the averaged result of eight naive observers. For this and subsequent figures, if error bars are absent from selected symbols the standard errors are smaller than the sizes of the symbols.

significant correlation exists between both measures ($R^2 = 0.9018$, $P < 0.001$), indicating that a common piece of perceptual information[6], namely the perceived surface slant due to the reduced view of the ground, might affect both types of space judgement. The perceived surface slant and its consequence for judged target distance (Fig. 2a, b) probably reflect the weighted contributions of the restricted texture information on the ground and the intrinsic bias of the visual system in representing the ground surface. (Measuring the implicit slant errors in the dark, in which the observer has no access to ground texture information, reveals the latter[3].) It is reasonable to suggest that when the visual field size increases, the relative contribution of ground texture information to the ground-surface representation mechanism increases. This, then, improves the accuracy of representing the ground surface, and hence distance.

Evidently, distance judgements improve with larger field sizes, because the visual system is able to access more visual surface information for representing the ground. But which part of the ground holds more essential information? To answer this in Experiment 3, we compared absolute distance judgement when the visual field was delimited vertically and horizontally. The observers, without head movements, wore a pair of goggles with a vertical rectangular aperture that maintained the vertical field at 50.9° while restricting the horizontal view. Figure 3a shows that the averaged blind-walking performances were as accurate as in the full-view condition (control) for all three aperture-size conditions ($F(4,28) = 0.143$, $P = 0.965$; $F(12,84) = 0.863$, $P = 0.586$). The observers were also tested with horizontal apertures that maintained the horizontal view at 57.7° while restricting the vertical view. The averaged results (Fig. 3b) show that absolute distance judgements with the 39.9° and 29.6° vertical field extents were as accurate as that in the full-view condition (39.9°: $F(1,7) = 1.473$, $P = 0.264$; $F(3,21) = 6.591$, $P < 0.001$; 29.6°: $F(1,7) = 4.151$, $P = 0.081$; $F(3,21) = 2.784$, $P = 0.066$); however, distances were underestimated when the vertical field extents were reduced to 21.1° ($F(1,7) = 27.220$, $P < 0.001$; $F(3,21) = 1.364$, $P = 0.291$] and 13.6° [$F(1,7) = 69.420$, $P < 0.001$; $F(3,21) = 1.207$, $P = 0.332$). Our data indicate that for a target distance of 4 m and an average eye height of 1.67 m, the 21.1° vertical aperture blocked the view of the near ground surface up to about 2.55 m from the observer. Clearly, the near ground surface, which provides reliable depth information, is critical for representing the ground.

The findings of Experiment 3 underscore the necessity for the visual system to make use of not only the far ground around the target, but also the near-ground information[18,19]. This suggests that representing the ground surface requires integrating local patches of ground surface from the observer to the target. Further, it can be surmised that the near-ground information serves as a foundation early on in the surface representation process, rather than late, to guarantee an accurate representation. Experiment 4 proves this by comparing absolute distance performances when observers were asked to scan the visual scene from the near to the far ground surface (near-to-far), in comparison with the reverse scanning direction (far-to-near). To scan the entire grass field while viewing through the aperture, the observer rotated his head once either upward from an initial downward head position (near–far-1 scanning), or

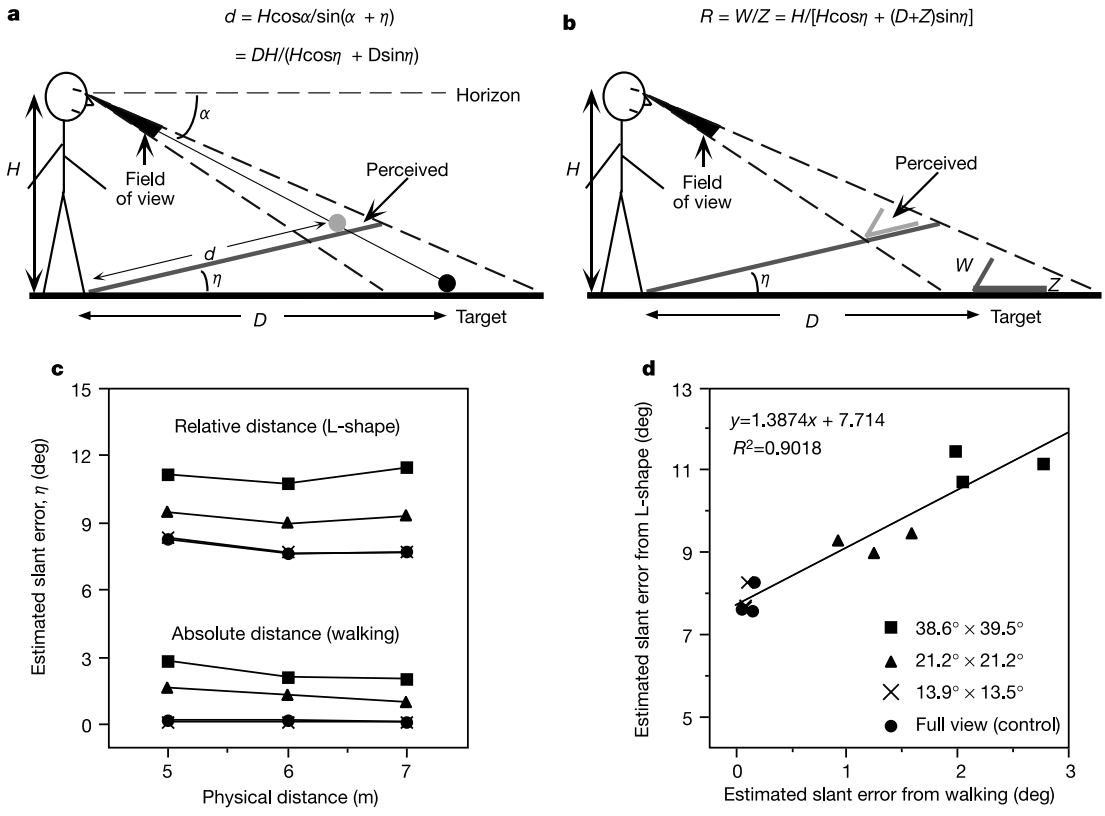


**Figure 2** Profile illustrations of the physical and perceived ground surface through a limited field of view. **a**, **b**, A flat ground surface (black line) is visually represented as a slant surface (grey line) with a slant error of $\eta$. **a**, An observer with an eye height of $H$ perceives a target (black disk) on the flat ground as one (grey disk) on the slant surface. As the perceived target's angular declination ($\alpha$) remains correct, the perceived target distance, $d$, is determined by the equation above the figure. **b**, Similarly, the grey L-shaped target on the flat ground is perceived as one (lighter grey) on the slant surface. The perceived relative length-in-depth is defined by the perceptual aspect ratio, $R = W/Z$, and is governed by the equation above the figure. **c**, Slant errors ($\eta$) are derived from the blind-walking and perceptual matching (L-shaped) data using the equations in **a** and **b**, respectively. The graph relates the estimated slant error to the physical distance. **d**, For each physical distance tested, the estimated slant errors from the relative length-in-depth (L-shaped) and absolute distance (blind-walking) tasks are related in the scatter plot.

downward from an initial straight-ahead position (far–near-1 scanning). Figure 4 shows the averaged blind-walking results from two different aperture sizes, where open triangles depict performance for near-to-far, and filled triangles show performance for far-to-near. Clearly, the latter was underestimated whereas the former remained as accurate as in the full-view condition ($57.7° \times 13.6°$ aperture: $F(1,7) = 19.759$, $P < 0.005$; $F(3,21) = 12.355$, $P < 0.001$; $57.7° \times 21.1°$ aperture: $F(1,7) = 41.429$, $P < 0.001$; $F(3,21) = 14.362$, $P < 0.001$). These results indicate that accurate surface representation is obtained through surface integration, and only when the near ground surface is accessed before the far.

However, perhaps for lack of iteration, the visual system was unable to form an accurate surface representation with only one chance to scan from the far ground to near. We therefore asked the observers to scan twice. In a far–near-2 condition, the observer rotated his head downwards to scan from the far ground to near, then pulled a blindfold over his goggles and repositioned his head (straight), removed the blindfold, and rotated his head downward to scan from far to near again, before performing the blind-walking task. For completeness, we included a near–far-2 condition in which scanning from near to far was performed twice. The filled squares in Fig. 4 represent the far-to-near scanning performances, which were underestimated in comparison with the near-to-far scanning performances (open squares) ($57.7° \times 13.6°$ aperture: $F(1,7) = 18.642$, $P < 0.005$; $F(3,21) = 11.804$, $P < 0.001$; $57.7° \times 21.1°$ aperture: $F(1,7) = 22.087$, $P < 0.005$; $F(3,21) = 6.759$, $P < 0.005$). Altogether, finding that scanning twice in the 'wrong' direction (far–near-2) did not improve performance suggests strongly that the visual representation of the near ground serves as an anchor, or foundation, early on in the surface representation process to build an accurate representation.

We conducted a control experiment to negate the possibility that the asymmetric performance in Experiment 4 was due to the motor system responsible for head movement. We compared blind-walking performances in judging the location (distance and height) of a light target[3] in three viewing conditions (free head motion, near-to-far head motion, and far-to-near head motion) in the dark, where other visual cues are unavailable (see Methods). The observers performed similarly in all three conditions, indicating that without a visible ground surface the scanning direction is irrelevant (distance: $F(2,14) = 0.764$, $P = 0.484$; $F(6,42) = 1.664$, $P = 0.154$; height: $F(2,14) = 2.613$, $P = 0.109$; $F(6,42) = 0.882$, $P = 0.517$). The asymmetry in Experiment 4 therefore reveals the process of representing visual surface information.

In summary, our findings reveal that for accurate distance judgement the human visual system relies on a surface integration process to form a global ground-surface representation, which is used as a reference frame for coding distances[3,8,14,19,20]. The surface integration process has a directional dictate, from near to far, for it to use the reliable visual depth information on the near ground surface. Furthermore, having the observer sample local patches of texture information by scanning reminds us of a parallel in nature.

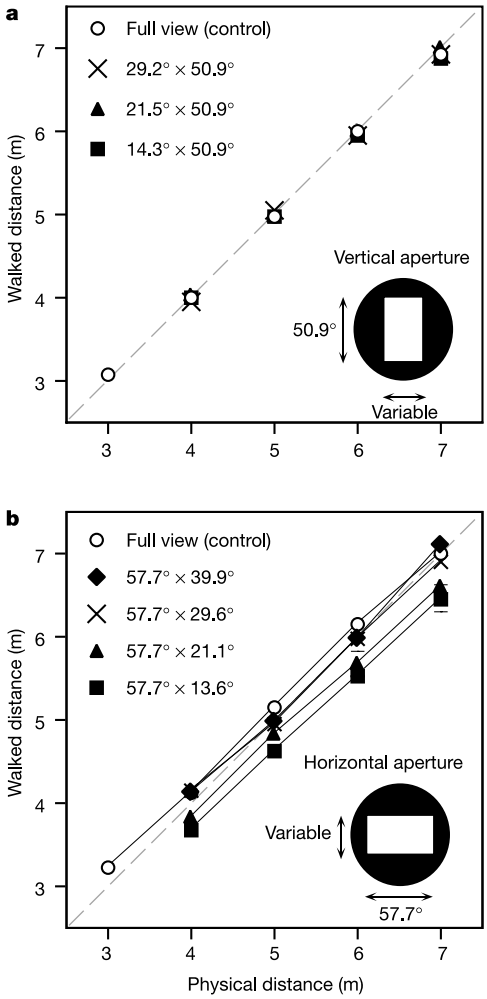


**Figure 3** The critical ground surface for accurate distance judgement. Comparison of the impact of vertical (**a**) and horizontal (**b**) rectangular apertures on the judged absolute distance measured with the blind-walking task. Each symbol represents the averaged result of eight naive observers.

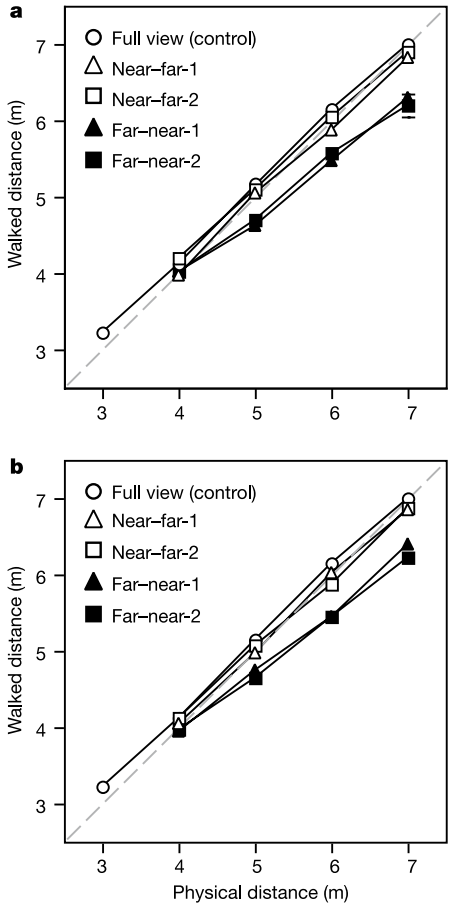


**Figure 4** Scanning direction affects judged absolute distance. **a**, **b**, Data from the $57.7° \times 13.6°$ (**a**) and $57.7° \times 21.1°$ (**b**) aperture-size experiments. Each symbol represents the averaged result of eight naive observers.

In particular, lower animals with few photoreceptor cells—and therefore very limited visual fields—use scanning to detect objects and to learn or recognize landmarks beyond their visual field coverage[21,22]. In humans, scanning local information with the fovea during surface integration also ensures that the information sampled has better spatial resolution than that afforded by the peripheral retina[22]. □

## Methods

### Observers

Ten naive observers with self-reported normal vision and informed consent participated in the various experiments. All performed the experiments with their motor dominant, right eye. To limit the monocular field of view to a preselected size, a pair of clear safety goggles was painted black all over except for a rectangular area (aperture) in front of the right eye with the appropriate field extent. For all aperture sizes used, the observers were unable to see their body and feet without rotating their heads. The goggles were worn throughout the experiments except during the full-view (control) condition, in which the observers wore an opaque patch over the left eye without the goggles. They were not given any feedback about their performances.

### Judging absolute distance by using the blind-walking task

The observer previewed an orange–red disk target (7.62 cm in diameter and 2.54 cm high) on a flat grass surface and judged its absolute distance. Then he pulled a blindfold over his eyes (goggles) and walked forward to traverse the remembered target distance. He stopped upon reaching the remembered target location and remained there to allow the experimenter to measure the walked distance. Thereafter, the experimenter led the observer, still in blindfold, back to the starting point to ready for a new trial. Four target distances (4, 5, 6 and 7 m) were tested in a randomized order. Each distance was tested twice and the average was taken as the final result.

### Judging relative length-in-depth by using a perceptual matching task

Two white pipes, 3 cm in diameter, were used to construct the L-shaped target. The frontoparallel arm ($W$) of the L-shaped target was fixed at 40.5 cm, and the length of the arm in depth ($Z$) was adjustable. During a trial, the observer kept his head still and judged whether the width of arm-$Z$ was equal to the length of arm-$W$. If not, the observer pulled a blindfold over his eyes (goggles) and instructed the experimenter to adjust the length of arm-$Z$. After the experimenter finished making the adjustment and had walked away from the L-shaped target, the observer was told to remove the blindfold and to compare the width and length of the L-shaped target again. This was repeated several times until the observer was satisfied that the two arms matched in width and length. The base of the L-shaped target to the observer defined the viewing distance, which was one of three distances (5, 6 and 7 m) that was measured in a randomized order. Each distance was tested twice and the average was taken as the final result.

### Judging distance in the dark

The test target, a 0.23° internally illuminated red table tennis ball, was placed at one of four distances (2.50, 3.75, 5.00 and 6.25 m) either on the floor or 0.5 m above it. Trials with targets above the floor served as catch trials (one-third of the total trials). Other than the test target, the room was completely dark so that the observer could not access other visual cues. For each trial, the observer ($n = 9$) previewed the distance and height of the target with the dominant eye. After this, the target was extinguished and the observer walked blindly to the remembered target location. Upon reaching his destination, the observer gestured the perceived height of the remembered target with his hand. The walked distance and gestured height are taken as the judged distance and height of the target, respectively. This procedure was used for all three conditions tested (free head motion, near-to-far head motion and far-to-near head motion).

### Data analysis

We applied the two-way analysis of variance with repeated-measures analysis to our data to obtain the $F$ and $P$ values indicated in the text. Following convention, the main effect and interaction are presented in order.

Received 12 August 2003; accepted 20 January 2004; doi:10.1038/nature02350.


1. Gogel, W. C. & Tietz, J. D. A comparison of oculomotor and motion parallax cues of egocentric distance. *Vision Res.* **19,** 1161–1170 (1979).
2. Philbeck, J. W. & Loomis, J. M. Comparison of two indicators of perceived egocentric distance under full-cue and reduced-cue conditions. *J. Exp. Psychol. Hum. Percept. Perform.* **23,** 72–85 (1997).
3. Ooi, T. L., Wu, B. & He, Z. J. Distance determined by the angular declination below the horizon. *Nature* **414,** 197–200 (2001).
4. Thomson, J. A. Is continuous visual monitoring necessary in visually guided locomotion? *J. Exp. Psychol. Hum. Percept. Perform.* **9,** 427–443 (1983).
5. Rieser, J. J., Ashmead, D., Talor, C. & Youngquist, G. Visual perception and the guidance of locomotion without vision to previously seen targets. *Perception* **19,** 675–689 (1990).
6. Loomis, J., DaSilva, J., Fujita, N. & Fukusima, S. Visual space perception and visually directed action. *J. Exp. Psychol.* **18,** 906–921 (1992).
7. Loomis, J., DaSilva, J., Philbeck, J. W. & Fukusima, S. Visual perception of location and distance. *Curr. Dir. Psychol. Sci.* **5,** 72–77 (1996).
8. Sinai, M. J., Ooi, T. L. & He, Z. J. Terrain influences the accurate judgement of distance. *Nature* **395,** 497–500 (1998).
9. Loomis, J. M. & Knapp, J. M. in *Virtual and Adaptive Environments* (eds Hettinger, L. J. & Hass, M. W.) 21–46 (Erlbaum, Hillsdale, New Jersey, 2003).
10. Hagen, M. A., Jones, R. K. & Reed, E. S. On a neglected variable in theories of pictorial perception: Truncation of the visual field. *Percept. Psychophys.* **23,** 326–330 (1978).
11. Dolezal, H. *Living in a World Transformed: Perceptual and Performatory Adaptation to Visual Distortion* (Academic, New York, 1982).
12. Loomis, J. M. & Philbeck, J. W. Is the anisotropy of perceived 3-D shape invariant across scale? *Percept. Psychophys.* **61,** 397–402 (1999).
13. Loomis, J. M., Philbeck, J. W. & Zahorik, P. Dissociation of location and shape in visual space. *J. Exp. Psychol. Hum. Percept. Perform.* **28,** 1202–1212 (2002).
14. Gibson, J. J. *The Perception of the Visual World* (Houghton, Mifflin, Boston, Massachusetts, 1950).
15. Gibson, J. J. The perception of visual surfaces. *Am. J. Psychol.* **63,** 367–384 (1950).
16. Freeman, R. B. Jr Effect of size on visual slant. *Psychol. Rev.* **72,** 501–504 (1956).
17. Braunstein, M. L. Motion and texture as sources of slant information. *J. Exp. Psychol.* **78,** 247–253 (1968).
18. Gibson, J. J. & Cornsweet, J. The perceived slant of visual surfaces—optical and geographical. *J. Exp. Psychol.* **44,** 11–15 (1952).
19. Sedgwick, H. A. in *Handbook of Perception and Human Performance* (eds Boff, K. R., Kaufman, L. & Thomas, J. P.) 21.1–21.57 (Willey, New York, 1986).
20. Meng, J. C. & Sedgwick, H. A. Distance perception mediated through nested contact relations among surface. *Percept. Psychophys.* **63,** 1–15 (2001).
21. Land, M. F. Scanning eye movements in a heteropod mollusc. *J. Exp. Biol.* **96,** 427–430 (1982).
22. Land, M. F. Motion and vision: why animals move their eyes. *J. Comp. Physiol. A* **185,** 341–352 (1999).


**Acknowledgements** This research was supported in part by a grant from NIH to Z.J.H. and T.L.O. and by a RIG grant from the University of Louisville to Z.J.H.

**Competing interests statement** The authors declare that they have no competing financial interests.

**Correspondence** and requests for materials should be addressed to Z.J.H. (zjhe@louisville.edu) or T.L.O. (tlooi@pco.edu).

# Inactivation of *hCDC4* can cause chromosomal instability

**Harith Rajagopalan[1], Prasad V. Jallepalli[1,2], Carlo Rago[1], Victor E. Velculescu[1], Kenneth W. Kinzler[1], Bert Vogelstein[1,3] & Christoph Lengauer[1]**

[1]*The Sidney Kimmel Comprehensive Cancer Center, Johns Hopkins University School of Medicine, Baltimore, Maryland 21231, USA*
[2]*Molecular Biology Program, Memorial Sloan-Kettering Cancer Center, New York, New York 10021, USA*
[3]*Howard Hughes Medical Institute, The Johns Hopkins University Medical Institutions, Baltimore, Maryland 21231, USA*

**Aneuploidy, an abnormal chromosome number, has been recognized as a hallmark of human cancer for nearly a century[1]; however, the mechanisms responsible for this abnormality have remained elusive. Here we report the identification of mutations in *hCDC4* (also known as *Fbw7* or *Archipelago*) in both human colorectal cancers and their precursor lesions. We show that genetic inactivation of *hCDC4*, by means of targeted disruption of the gene in karyotypically stable colorectal cancer cells, results in a striking phenotype associated with micronuclei and chromosomal instability. This phenotype can be traced to a defect in the execution of metaphase and subsequent transmission of chromosomes, and is dependent on cyclin E—a protein that is regulated by hCDC4 (refs 2–4). Our data suggest that chromosomal instability is caused by specific genetic alterations in a large fraction of human cancers and can occur before malignant conversion.**

CDC4 is an evolutionarily conserved E3 ubiquitin ligase that is thought to be involved in regulating the G1–S cell-cycle checkpoint by targeting proteins for destruction by the SCF complex of proteins[2]. Mutations in the *hCDC4* gene were originally identified in a few breast and ovarian cancer cell lines and have been subsequently found in endometrial cancers[5–7]. Here we have